J Appl Physiol 126: 1074–1087, 2019.
First published January 24, 2019; doi:10.1152/japplphysiol.00582.2018.

RESEARCH ARTICLE | *Translational Control of Muscle Mass*

Reduced frequency of resistance-type exercise training promotes adaptation of the aged skeletal muscle microenvironment

Marshall A. Naimo,[1,2] Erik P. Rader,[1] James Ensey,[1] Michael L. Kashon,[1] and Brent A. Baker[1]

[1]*Health Effects Laboratory Division, National Institute for Occupational Safety and Health, Centers for Disease Control and Prevention, Morgantown, West Virginia; and* [2]*Division of Exercise Physiology, School of Medicine, West Virginia University, Morgantown, West Virginia*

Submitted 28 June 2018; accepted in final form 18 January 2019

Naimo MA, Rader EP, Ensey J, Kashon ML, Baker BA. Reduced frequency of resistance-type exercise training promotes adaptation of the aged skeletal muscle microenvironment. *J Appl Physiol* 126: 1074–1087, 2019. First published January 24, 2019; doi:10.1152/japplphysiol.00582.2018.—The purpose of this study was to characterize the growth and remodeling molecular signaling response in aged skeletal muscle following 1 mo of "resistance-type exercise" training. Male Fischer 344 × Brown Norway hybrid rats aged 3 (young) and 30 mo (old) underwent stretch-shortening contraction (SSC) loading 2 or 3 days/wk; muscles were removed 72 h posttraining. Young rats SSC loaded 3 (Y3x) or 2 days/wk (Y2x) adapted via increased work performance. Old rats SSC loaded 3 days/wk (O3x) maladapted via decreased negative work; however, old rats SSC loaded 2 days/wk (O2x) adapted through improved negative and positive work. Y3x, Y2x, and O2x, but not O3x, displayed hypertrophy via larger fiber area and myonuclear domains. Y3x, Y2x, and O2x differentially expressed 19, 30, and 8 phosphatidylinositol 3-kinase-Akt genes, respectively, whereas O3x only expressed 2. Bioinformatics analysis revealed that rats in the adapting groups presented growth and remodeling processes (i.e., increased protein synthesis), whereas O3x demonstrated inflammatory signaling. In conclusion, reducing SSC-loading frequency in aged rodents positively influences the molecular signaling microenvironment, promoting muscle adaptation.

NEW & NOTEWORTHY Decreasing resistance-type exercise training frequency in old rodents led to adaptation through enhancements in performance, fiber areas, and myonuclear domains. Modifying frequency influenced the molecular environment through improvements in phosphatidylinositol 3-kinase-Akt pathway-specific expression and bioinformatics indicating increased protein synthesis. Reducing training frequency may be appropriate in older individuals who respond unfavorably to higher frequencies (i.e., maladaptation); overall, modifying the parameters of the exercise prescription can affect the cellular environment, ultimately leading to adaptive or maladaptive outcomes.

adaptation; central nuclei; Fischer 344 × Brown Norway rats; growth and remodeling; stretch-shortening contractions

INTRODUCTION

Significant issues associated with aging, such as frailty and cachexia, are related to sarcopenia, typically defined as the age-related loss of skeletal muscle mass with concomitant weakness (19, 36). Thus, strategies aiming to improve muscle performance and muscle mass in older individuals should be pursued to improve functional capacity and decrease musculoskeletal disorders. Recently, age-related physical changes have been suggested to be modifiable by increased physical activity (14). Evidence for the pluripotent effects of exercise led both the American Medical Association and the American College of Sports Medicine to launch an initiative in 2007 called "Exercise is Medicine," a global initiative to translationally incorporate scientifically supported health benefits of physical exercise into our healthcare system (9). Despite the therapeutic potential and supporting evidence, how age-specific resistance exercise positively influences the total health of an individual across the lifespan is equivocal. Furthermore, the integrated physiological pathways involved in exercise-induced muscle adaptation are not fully understood.

The responses to "resistance-type exercise" training (RTET) can range from adaptation, defined as gains in muscle mass and performance, to maladaptation, characterized by an absence of muscle mass gains and diminished performance (16). Exercise training involving the use of stretch-shortening contractions (SSCs), a common type of contraction in which the muscle is activated before and during the initial stretch and subsequent shortening (36), has been particularly beneficial in elucidating the benefits of exercise training. For nearly two decades, our laboratory has utilized an in vivo rodent dynamometer to investigate the underlying mechanics of muscle adaptation to RTET (4, 17); this methodology allows for precise control of the biomechanical loading signature (i.e., frequency) and is minimally invasive. The combination of this methodology with the use of SSCs, as opposed to isometric or lengthening-only contractions, makes it a physiologically representative model for the longitudinal study of muscle adaptation to RTET. Using a noninjurious paradigm of SSCs previously designed by our laboratory (8 sets of 10 SSCs, 3 days/wk for 4.5 wk), RTET-induced adaptation occurs in young rodents (16); however, this response is altered with age. Specifically, results demonstrated that aged rodents undergo a maladaptive response when exposed to this protocol (5, 6, 16, 35, 36, 41). Similarly, other studies in older humans have also found a reduced capacity to adapt to resistance exercise training (37–39, 44). Moreover, a recent National Health and Nutrition Survey analysis showed statistical associations between sufficient levels of resistance training and greater muscle quality with select age groups at early old age but not at later old age

Address for reprint requests and other correspondence: B. A. Baker, Health Effects Laboratory Division, National Institute for Occupational Safety and Health, Centers for Disease Control and Prevention, 1095 Willowdale Road, MS-L3027, Morgantown, WV 26505-2888 (e-mail: bwb3@cdc.gov).

(30). These results, along with the studies mentioned above, indicate that as one gets older, appropriate age-specific exercise prescription may be a critical component that enables skeletal muscle adaptation in response to RTET.

In recent work by our laboratory, we investigated whether modulating the exercise prescription by reducing the training frequency from 3 to 2 days/wk resulted in decreased oxidative stress and enhanced muscle quality in older rodents to levels similar to those of young rats that adapted (36). These results indicate that additional recovery between training bouts may be beneficial for developing a favorable redox environment and subsequently promoting muscle adaptation (34). Protein kinase B (Akt) is a serine/threonine kinase that is a widely accepted key regulator of muscle growth (21). Activation of Akt has several downstream physiological outcomes, including roles in metabolism, protein synthesis, apoptosis, the regulation of transcription factors, and involvement in the cell cycle. Mechanical loading has been shown to cause increased activation of Akt independently of growth factors or nutrient stimulation through multiple mechanosensory molecules (26, 27). This suggests that SSC loading may directly modify Akt signaling during active RTET, possibly leading to an adaptive or maladaptive fate. Despite the well-known benefits of phosphatidylinositol 3-kinase (PI3K)-Akt signaling on the hypertrophic response to resistance exercise, no studies have examined the PI3K-Akt pathway response and determined the distinct molecular signature occurring with aging while connecting it to adaptive outcomes (i.e., force output and changes in muscle fiber area), particularly in a precisely controlled in vivo physiologically representative model of resistance exercise. Additionally, it is not known whether the PI3K-Akt pathway response is altered when parameters of the exercise prescription are manipulated in a manner that causes adaptation or maladaptation to occur. Therefore, the purpose of this study was to define and extend our previous findings by implementing an integrated systems biology approach using representative PI3K-Akt pathway gene expression and bioinformatics via Ingenuity Pathway Analysis (IPA), in addition to biochemical, morphological, as well as physiological muscle measures and muscle performance. Our hypothesis was that young rats would respond at the performance, physiological, and molecular level in an adaptive manner regardless of whether training frequency was reduced, whereas old rats trained at a higher frequency would have a blunted response indicative of maladaptation. Additionally, we hypothesized that old rats trained at a reduced frequency would have a molecular growth and remodeling response that more closely resembles that of younger rats that adapt following SSC training.

MATERIALS AND METHODS

Animals. Young (3 mo) and old (30 mo) male Fischer 344 × Brown Norway (F344xBN) rats were obtained from the National Institute of Aging colony and housed in Association for Assessment and Accreditation of Laboratory Animal Care International-accredited animal quarters. All animal procedures were approved by the Animal Care and Use Committee at the National Institute for Occupational Safety and Health in Morgantown, West Virginia, and were in compliance with the National Institutes of Health guide for the care and use of animals in research.

RTET paradigm. F344xBN male rats were randomly assigned to a high-intensity SSC RTET protocol for 4.5 wk in one of the following four groups: *1*) young rats SSC loaded 3 days/wk (Y3x; $n = 10$), *2*) young rats SSC loaded 2 days/wk (Y2x; $n = 10$), *3*) old rats SSC loaded 3 days/wk (O3x; $n = 10$), and *4*) old rats SSC loaded 2 days/wk (O2x; $n = 8$). Because of limited tissue availability, experiments that yielded the results in Figs. 2–4 were done on a subset of animals within each condition ($n = 4–6$ per group) rather than the entire experimental cohort. The loading paradigms were identical with the exception of the training frequency. For the 2 day/wk training groups, training was conducted on Mondays and Thursdays, with 72 h between training bouts. For the 3 day/wk training group, training was performed on Mondays, Wednesdays, and Fridays, with 48-h rest between training sessions. The training protocol was based on a previously validated, SSC RTET protocol (16, 17, 36). Briefly, rats were anesthetized with isoflurane gas and placed in dorsal recumbency on a heated table with the left knee secured in flexion at 90° and the left foot secured in a load cell. Platinum electrodes were then placed subcutaneously for activation of the dorsiflexor muscles. Muscle stimulation parameters (4-V magnitude, 0.2-ms pulse duration, and 120-Hz frequency) were based on previous studies of this model that found these settings to be optimal for producing supramaximal force outputs of the tibialis anterior (TA) muscle in male rats (16, 17). Training consisted of 80 total SSCs per session, which comprised 8 sets of 10 repetitions, with 2-min rest intervals between sets. For every SSC, the muscles were maximally activated, with the ankle set to 90° for 100 ms, rotated out to 140° at a movement velocity of 60°/s, and then returned to 90° at 60°/s. Using this protocol, age-specific performance adaptation occurs with a concomitant absence of overt muscle inflammation and degeneration in the days and weeks following training (5, 6, 16, 36).

During each training session, muscle performance was assessed during the first SSC repetition of the first training set. Both the work required to stretch the muscle (i.e., negative work) and the work performed by the muscle during the shortening phase (i.e., positive work) were measured and recorded using MATLAB software (version 9.3; The MathWorks, Natick, MA). Seventy-two hours after the final SSC-loading protocol, rats were euthanized, and the TA muscle was surgically removed, weighed, and recorded as the raw muscle mass (i.e., wet weight) in grams. This length of time (72 h) was chosen because this would be beyond the acute effects of first several hours posttraining, but within the timeline where any overt signs of muscle degeneration as a consequence of the last training session would occur (36). The midbelly of the TA muscle was coated with tissue-freezing media (Tissue-Tek, 4583 O.C.T. Compound; Sakura Finetek, Torrance, CA) and frozen in isopentane (−80°C) for quantitative morphology. The remaining TA muscle was allocated for gene expression and protein analysis.

Muscle fiber area, myonuclear count, and myonuclear domain. Frozen TA muscle sections (12-μm thickness) were previously stained for 4-hydroxynonenal (no. 393206, at 1:250; Calbiochem, La Jolla, CA), β-dystroglycan (sc-33701, at 1:100; Santa Cruz Biotechnology, Dallas, TX) to outline the muscle sarcolemma, and 4′,6-diamidino-2-phenylindole (P-36931; Thermo Fisher Scientific, Rockville, IL) stain for myonuclei, and representative images were reported elsewhere (36). The midpoint of the TA muscle was identified, and nonoverlapping images were captured at ×40 magnification at the site of most area in both the lateral and medial regions of the TA muscle section. A standardized stereological method was used for quantitative morphology (7). Briefly, at two regions (1 mm to the right and 1 mm to the left of the section midline) the analysis was performed at five equally spaced sites across the muscle section. At each site, points of a 121-point, 11-line overlay graticule (0.04-mm^2 square boundary with 100 divisions) were placed at the center of each image and were used to count various features, which included muscle fibers and myonuclei. A total of 1,210 points were analyzed per section since 10 total fields (i.e., images) were evaluated.

The investigator was blinded to sample identity, and samples were analyzed utilizing ImageJ (version 1.48; National Institutes of Health,

Bethesda, MD). Each muscle fiber (208 ± 21 fibers per section, mean ± SE) was traced to determine muscle fiber area. Myonuclei were manually counted within the sarcoplasm regions of muscle sections. The number of myonuclei per unit of muscle cross-sectional area (nuclei per mm^2) was determined by dividing the number of myonuclei by the total muscle fiber area sampled. The percentage of central nucleated fibers (CNFs) was quantified by dividing the number of muscle fibers that presented with central nuclei by the total number of muscle fibers sampled. Myonuclear domain (MND), typically defined as the volume unit of which the transcriptional activity level of a muscle fiber is under the direct control of a single myonucleus (15), was quantified as the ratio of the muscle fiber area relative to the number of myonuclei for each myofiber.

Gene expression analysis. Muscle tissue stored at −80°C was retrieved, and then a 50-mg portion was homogenized using a Mini-Beadbeater-8 (BioSpec Products, Bartlesville, OK) with 1 ml TRIzol and 1.0-mm zirconia beads (cat. no. 22079110zx; BioSpec). RNA was subsequently isolated using the RNAqueous phenol-free total RNA isolation kit (cat. no. AM-1912; Thermo Fisher Scientific) following kit instructions. Next, cDNA was synthesized using the RT^2 First Strand Kit (cat. no. 330401; Qiagen). Samples were then analyzed using the rat skeletal muscle PI3K-AKT Signaling Pathway RT^2 Profiler PCR Array (cat. no. PARN-058Z; Qiagen) and RT^2 SYBR Green Mastermix (cat. no. 330523; Qiagen) per manufacturer's instructions with use of an ABI PRISM 7500 instrument (Applied Biosystems, Foster City, CA). The RT^2 Profiler PCR array was able to simultaneously assay 84 genes related to the PI3K-Akt signaling pathway (Table 1). Fold changes and *P* values were determined from comparisons of normalized cycle threshold (ΔC_t) values between SSC-loaded and nonloaded control (NLC) muscles (i.e., the contralateral limb that was not subjected to RTET) and analyzed through the GeneGlobe Data Analysis Center (Qiagen). Bioinformatics analysis was performed using IPA (Ingenuity Systems, https://www.ingenuity.com/), which allowed for functional annotation of differentially expressed genes. All IPA biological functions except cancer-specific, reproductive system, and psychological functions were evaluated.

Total RNA, DNA, and protein. RNA was isolated following the protocol outlined in MATERIALS AND METHODS, *Gene expression analysis*. Total DNA was isolated using the DNeasy Blood & Tissue Kit (Qiagen) according to kit instructions. Both RNA and DNA concentrations were obtained using a spectrophotometer (ND-1000; NanoDrop Technologies, Wilmington, DE). Cytoplasmic protein isolation extracts were obtained from the TA muscles using a method described by Siu et al. (43). Total protein contents of the cytoplasmic protein extracts were quantified and reported as protein concentration ([protein]; μg protein/mg tissue) in triplicate using the Pierce BCA Protein Assay Kit (Thermo Scientific). Additionally, values for the [RNA]-to-[DNA] ratio (i.e., assumed to be a surrogate measure of global transcriptional efficiency) and the [protein]-to-[RNA] ratio (i.e., assumed to be a surrogate measure of global translational efficiency) were analyzed (40).

Statistical analysis. Negative work, positive work, myonuclear count, muscle RNA, muscle DNA, muscle protein, muscle transcriptional efficiency, and muscle translational efficiency were all analyzed using a mixed-model analysis of variance with the variable of animal identification as a random factor to account for repeated measures (JMP version 11; SAS Institute, Cary, NC). PI3K-Akt PCR data were analyzed using unpaired Student's *t*-test in the GeneGlobe Data Analysis Center (Qiagen) online platform. χ^2-Analysis (SigmaPlot version 12.5; Systat Software, San Jose, CA) was utilized to determine training-induced differences in the absolute frequency distributions of muscle fiber area and MND. All data are expressed as means ± SE, with $P < 0.05$ being considered statistically significant.

RESULTS

Dorsiflexor muscle performance. Negative work performed on the first SSC repetition of the first training set during the initial and final weeks of training is shown in Fig. 1*A*. In response to dorsiflexion SSC loading, Y3x and Y2x adapted to SSC training as indicated by significantly higher negative work following training (387 ± 15 to 484 ± 26 N and 395 ± 20 to 489 ± 30 N, respectively; $P < 0.01$), whereas O3x had significantly decreased negative work (343 ± 20 to 277 ± 29 N; $P < 0.05$). Meanwhile, O2x had a trend for increased negative work following training (328 ± 7 to 392 ± 31 N; $P = 0.07$). For positive work, Y3x had a trend for a higher initial value relative to O3x (296 ± 20 vs. 240 ± 21 N; $P = 0.08$), whereas Y2x had significantly higher initial results compared with O2x (303 ± 23 vs. 210 ± 15; $P < 0.05$; Fig. 1*B*). Following training, only O3x had significantly decreased positive work (240 ± 21 to 174 ± 24 N; $P < 0.05$). Furthermore, Y3x (317 ± 26 N; $P < 0.0001$) and Y2x (323 ± 22 N; $P < 0.0001$), as well as O2x (241 ± 23 N; $P < 0.05$), exhibited significantly higher positive work than did O3x (174 ± 24 N).

Muscle mass, fiber area, myonuclear count, central nuclei, and MND. No differences were found between young and old NLC raw muscle mass (585 ± 13 vs. 572 ± 24 mg; $P > 0.05$).

Table 1. *PI3K-AKT Signaling Pathway RT^2 Profiler PCR Array*

	Column											
Row	*1*	*2*	*3*	*4*	*5*	*6*	*7*	*8*	*9*	*10*	*11*	*12*
A	Adar	Akt1	Akt2	Akt3	Apc	Bad	Btk	Casp9	Ccnd1	Cd14	Cdc42	Cdkn1b
B	Chuk	Csnk2a1	Ctnnb1	Eif2ak2	Eif4b	Eif4e	Eif4ebp1	Eif4g1	Faslg	Fkbp1a	Fos	Foxg1
C	Foxo3	Gja1	Grb10	Grb2	Gsk3b	Hras	Hspb1	Igf1	Igf1r	Ilk	Irak1	Irs1
D	Itgb1	Jun	Kcnh8	Map2k1	Mapk1	Mapk14	Mapk3	Mapk8	Mtcp1	Mtor	Myd88	Nfkb1
E	Nfkbia	Pabpc1	Pak1	Pdgfra	Pdk1	Pdk2	Pdpk1	Pik3ca	Pik3cg	Pik3r1	Pik3r2	Prkca
F	Prkcb	Prkcz	Pten	Ptk2	Ptpn11	Rac1	Raf1	Rasa1	Rbl2	Rheb	Rhoa	Rps6ka1
G	Rps6kb1	Shc1	Sos1	Srf	Tcl1a	Tirap	Tlr4	Tollip	Tsc1	Tsc2	Wasl	Ywhah
H	Actb	B2m	Hprt1	Ldha	Rplp1	RGDC	RTC	RTC	RTC	PPC	PPC	PPC

Actb, β-actin; Adar, adenosine deaminase RNA specific, Apc, Apc regulator of Wnt signaling pathway, B2m, β2-microglobulin; Btk, Bruton tyrosine kinase; Casp9, caspase 9; Ccnd1, cyclin D1; Eif2ak2, eukaryotic translation initiation factor 2α kinase 2; Faslg, Fas ligand; Foxg1, forkhead box G1; Gja1, gap junction protein-α1; Hprt1, hypoxanthine phosphoribosyltransferase 1; Igf1r, IGF-1 receptor; Irak1, IL-1 receptor-associated kinase 1; Kcnh8, potassium voltage-gated channel subfamily H member 8; Ldha, lactate dehydrogenase A; Myd88, Myd88 innate immune signal transduction adaptor; Nfkb1, NF-κB subunit 1; Nfkbia, NF-κB inhibitor-α; Pdgfra, PDGF receptor-α; PI3K, phosphatidylinositol 3-kinase; Pik3ca and Pik3g, phosphatidylinositol-4,5-bisphosphate 3-kinase catalytic subunit-α and -γ, respectively; Pik3r1 and Pik3r2, phosphoinositide 3-kinase regulatory subunit 1 and 2, respectively; PPC, positive PCR control; Rasa1, Ras p21 protein activator 1; RGDC, rat genomic DNA contamination; Rhoa, Ras homolog family member A; Rplp1, ribosomal protein lateral stalk subunit P1; RTC, reverse transcription control; Shc1, Shc adaptor protein 1; Tcl1a, T cell leukemia/lymphoma 1A. See Table 3 for additional gene descriptors.

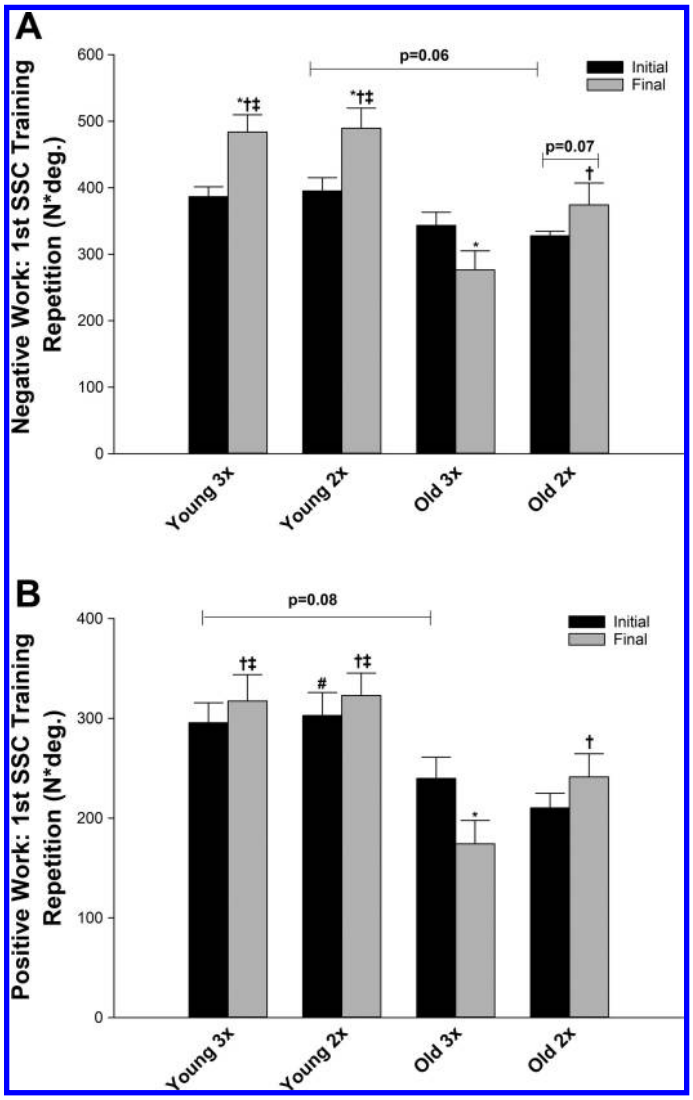

Fig. 1. Reduced frequency of stretch-shortening contraction (SSC) "resistance-type exercise" training improves muscle performance of aged rats. During each training session, tibialis anterior muscle performance was assessed during the first SSC repetition of the first training set. Both the work required to stretch the muscle (i.e., negative work) and the work performed by the muscle during the shortening phase (i.e., positive work) were measured, and values of dorsiflexion dynamic performance in terms of negative work performed on the first repetition of the first training set of each training session (*A*) and positive work performed on the first repetition of the first training set of each training session (*B*) were recorded. For each group, the work performed was averaged on the basis of recorded force values during the first week (initial) and last week of training (final). Sample sizes were $n = 8–10$ per group. Data are presented as means ± SE. *Different from initial, $P < 0.05$; #different from initial for old rats trained 2 days/wk, $P < 0.05$; †different from final for old rats trained 3 days/wk, $P < 0.05$; ‡different from final for old rats trained 2 days/wk, $P < 0.05$.

All four groups had significantly increased raw muscle mass following the SSC-loading training period (Y3x, 720 ± 29 mg; Y2x, 679 ± 67 mg; O3x, 610 ± 42 mg; O2x, 666 ± 32 mg; $P < 0.01$). Additionally, Y3x, Y2x, and O2x had significantly higher muscle mass compared with O3x following training ($P < 0.05$). Frequency distributions for muscle fiber areas are shown in Fig. 2. Following training, χ^2-analysis of muscle fiber area distributions revealed that there were significantly increased fiber areas for Y3x, Y2x, and O2x relative to NLC muscle ($P < 0.001$; Fig. 2, *A*, *B*, and *D*), whereas no changes were found in O3x ($P > 0.05$; Fig. 2*C*).

Myonuclear counts and percentage CNF results are shown in Table 2. Old NLC muscle had significantly higher myonuclear count relative to young NLC muscle ($P < 0.05$); there were no effects of 3 or 2 day/wk loading on myonuclear counts in any group. Similar to myonuclear count, the percentage of CNFs was significantly higher in old compared with young NLC muscle ($P < 0.05$). Following SSC loading, the percentage of CNFs was significantly lower in O3x compared with old NLC muscle ($P < 0.05$). Both young and old rats SSC loaded 2 days/wk had a significantly higher percentage of CNFs relative to age-matched counterparts ($P < 0.05$). MND was calculated by dividing muscle fiber area by the number of myonuclei for that myofiber (Fig. 3). When looking at each SSC-loaded group relative to age-matched NLC muscle, all groups except for O3x had a significant increase in their respective MNDs following training, particularly for O2x ($P < 0.001$; Fig. 3, *A–D*).

PI3K-Akt gene expression and bioinformatics analysis. The significantly differentially expressed genes (SDEGs) in the rat skeletal muscle PI3K-AKT Signaling Pathway RT^2 Profiler PCR Array are shown in Table 3 and Fig. 4 and are defined as having a P value <0.05. Y3x and Y2x had 19 and 30 SDEGs, respectively, in the PI3K-Akt signaling pathway. In contrast, O3x only had two SDEGs; however, O2x had eight SDEGs for the PI3K-Akt signaling pathway, a fourfold increase. Intriguingly, integrin-β1 (*Itgb1*), a key regulator of mechanotransduction signaling events in skeletal muscle in response to exercise (10), was significantly upregulated in both Y3x and Y2x, as well as in O2x (1.53-fold vs. 1.95-fold vs. 2.34-fold), whereas there was only a trend for upregulation in O3x. Additionally, FBJ osteosarcoma oncogene (*Fos*) and Jun oncogene (*Jun*), two important regulators of satellite cell activation (2), were significantly upregulated in O2x (*Fos*, 6.3-fold; *Jun*, 1.6-fold).

Bioinformatics analysis via IPA revealed several differential patterns when comparing between the adapting groups versus the O3x maladapted group (Table 4). For the top canonical pathways, Y3x, Y2x, and O2x had processes mainly associated with growth and remodeling events in muscle [e.g., ERK/MAPK signaling, mechanistic target of rapamycin (mTOR) signaling, hepatocyte growth factor (HGF) signaling, and IGF-1 signaling], whereas old rats loaded 3 days/wk had processes mainly related to inflammatory signaling (e.g., IL-17A signaling and T cell signaling). When evaluating the top networks, Y3x and Y2x had networks related to growth and remodeling processes such as cellular movement, cell death and survival, etc. After the networks in the adapted groups were merged to generate top merged-network functions, the processes were reflective of events associated with growth and/or the stress response to exercise (e.g., apoptosis, carbohydrate metabolism, cell cycle, and protein synthesis). O3x had a lone represented top network, and because of this, merged-network function analysis was unable to be performed. Meanwhile, O2x had two top networks, and the top merged-network functions were similar to those of both young groups, with processes related to the growth response to exercise (e.g., protein expression, proliferation of fibroblasts, and angiogenesis).

Muscle RNA, DNA, and protein. Figure 5 displays skeletal muscle concentrations for RNA, DNA, and protein. There were

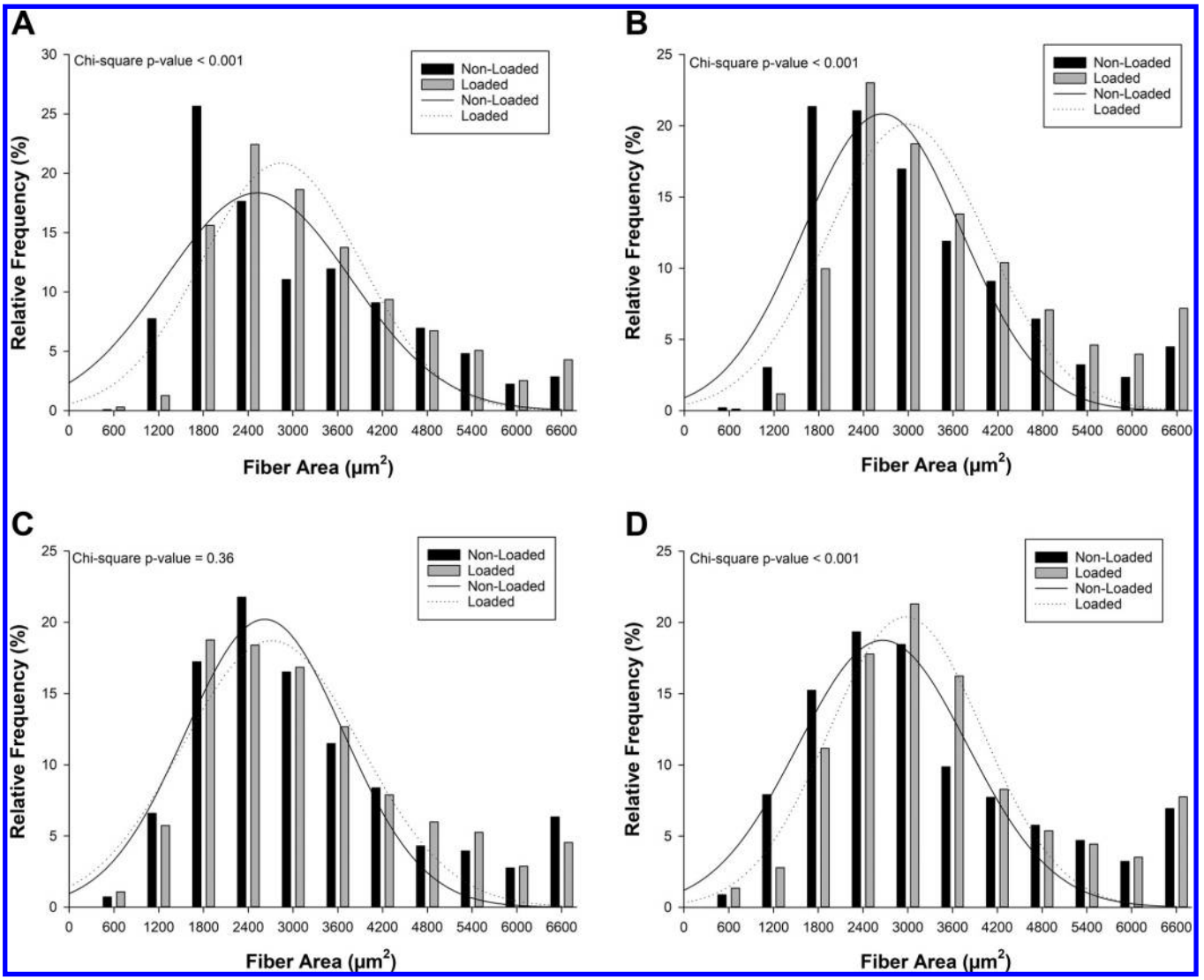

Fig. 2. Reduced frequency of stretch-shortening contraction (SSC) "resistance-type exercise" training increases tibialis anterior (TA) muscle mass size of aged rats. Frozen TA muscle sections stained for 4-hydroxynonenal and β-dystroglycan were manually traced to determine muscle fiber area. Frequency distributions for muscle fiber areas are presented as a percentage of the total myofibers measured for each group: young rats trained 3 days/wk (*A*), young rats trained 2 days/wk (*B*), old rats trained 3 days/wk (*C*), and old rats trained 2 days/wk (*D*). Sample sizes were $n = 4$–5 per group. Analyses were done comparing SSC-loaded muscle following resistance-type exercise training with age-matched nonloaded control TA muscle. All groups with the exception of old rats trained 3 days/wk demonstrated a significant shift in distribution toward a greater fiber area following training, $P < 0.05$.

no age or treatment effects for any group on muscle [RNA] ($P > 0.05$; Fig. 5*A*). For muscle [DNA], old NLC muscle had significantly higher concentrations compared with young NLC muscle ($P < 0.05$; Fig. 5*B*); additionally, Y3x and O2x had significantly increased muscle [DNA] compared with age-matched NLC muscle ($P < 0.05$). Moreover, O2x had significantly higher muscle [DNA] compared with Y2x ($P < 0.01$). For muscle [protein], old NLC's muscle [protein] was not different compared with that of young NLC muscle (Fig. 5*C*). For Y3x, there was a significant increase in [protein] compared

Table 2. *Quantitative myonuclear count and central nuclei for SSC-loaded and nonloaded control muscles of young and old rats*

	Young			Old		
	Nonloaded control	Loaded 3 days/wk	Loaded 2 days/wk	Nonloaded control	Loaded 3 days/wk	Loaded 2 days/wk
Myonuclear count, nuclei/mm^2	1,046 ± 51	1,031 ± 55	1,043 ± 99	1,223 ± 50*	1,155 ± 55	1,105 ± 26
Central nucleated fibers, %	7.3 ± 1.2	8.3 ± 2.2	14.3 ± 2.2†‡	12.5 ± 2.0*	4.3 ± 1.4†	15.1 ± 1.7‡

Values are means ± SE; n = no. of rats. Sample sizes were $n = 4$–5 per group. SSC, stretch-shortening contraction. *Different from value of the young nonloaded control muscle limb, $P < 0.05$; †different from value of the nonloaded control muscle within age, $P < 0.05$; ‡different from value of the trained limb for rats exposed 3 days/wk within age, $P < 0.05$.

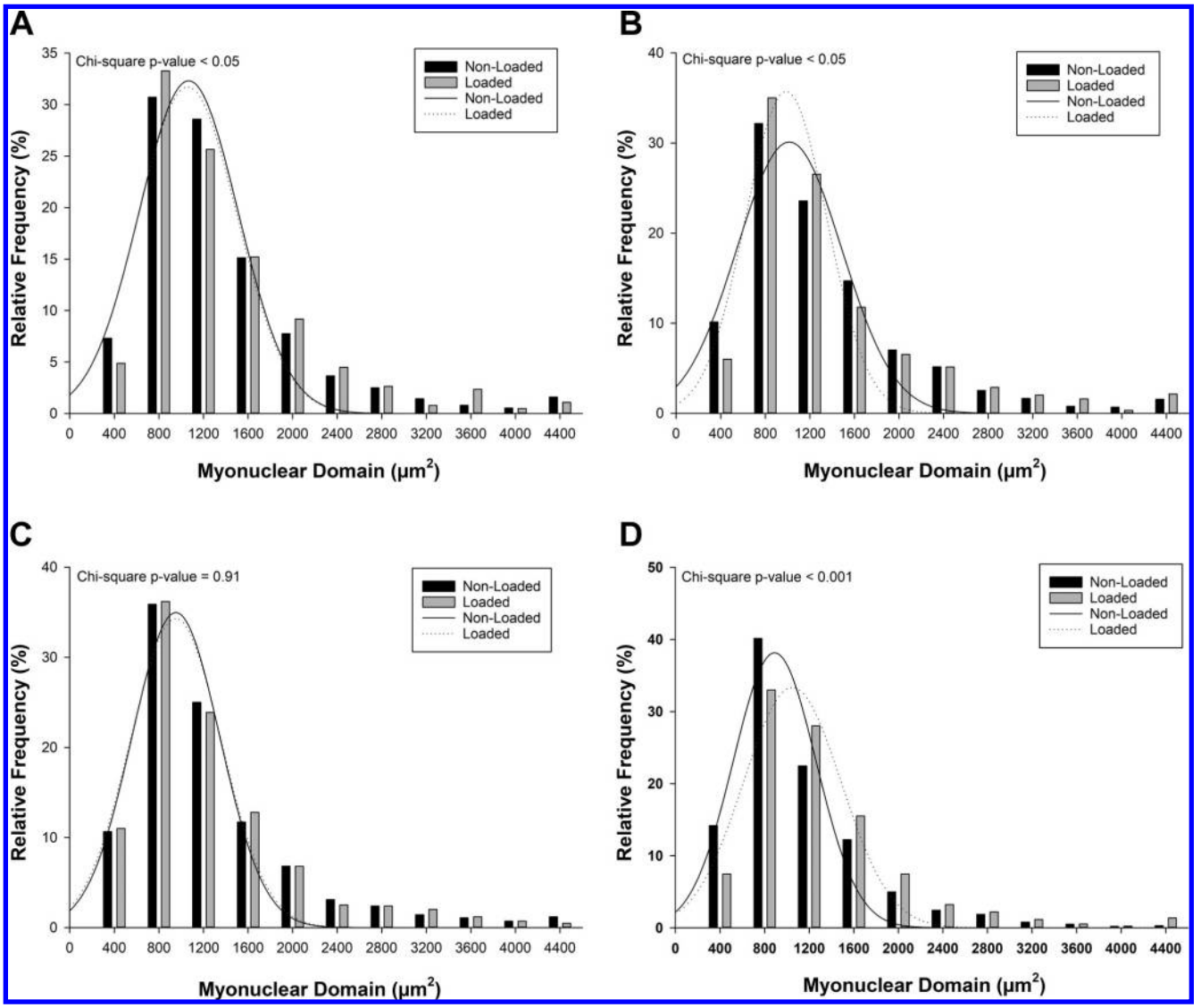

Fig. 3. Reduced frequency of stretch-shortening contraction (SSC) "resistance-type exercise" training increases the myonuclear domains of aged rats. Myonuclear domain was calculated as the ratio of the muscle fiber area relative to the number of myonuclei per myofiber and was quantified by dividing the number of myonuclei by the total muscle fiber area sampled (nuclei per mm^2). Frequency distributions for myonuclear domains are presented as a percentage of the total myonuclear domains measured for each group: young rats trained 3 days/wk (*A*), young rats trained 2 days/wk (*B*), old rats trained 3 days/wk (*C*), and old rats trained 2 days/wk (*D*). Sample sizes were $n = 4–5$ per group. Analyses were done comparing loaded muscle following SSC training with age-matched nonloaded control muscle. All groups with the exception of old rats trained 3 days/wk demonstrated a significant shift in distribution following training, $P < 0.05$. Note in particular the pronounced shift toward a higher myonuclear domain in the old rats trained 2 days/wk.

with Y2x ($P < 0.001$) and O3x ($P < 0.01$). O2x significantly increased muscle [protein] compared with old NLC muscle following training ($P < 0.01$). Strikingly, O2x also had significantly higher [protein] compared with O3x ($P < 0.01$) and Y2x ($P < 0.001$). Although there were no effects for surrogate muscle transcriptional efficiency index (Fig. 5*D*), there was a significantly higher surrogate muscle translational efficiency index in young compared with old NLC muscle ($P < 0.01$). There were no effects of SSC loading in the old rats ($P > 0.05$).

DISCUSSION

The main findings from this study are as follows: *1*) There is a distinct molecular signature following RTET utilizing SSCs in old rats that accompanies adaptive and maladaptive outcomes, and these responses appear to be connected to the PI3K-Akt signaling pathway, with SDEGs involved in muscle growth and remodeling present in both Y3x and Y2x, as well as O2x; *2*) effects on gene expression in O2x had a positive influence on downstream outcomes including central nucleation and increased MND; and *3*) this work advances recent work from our laboratory demonstrating the efficacy of a reduced-frequency exercise paradigm aiding the adaptability of aged muscle in response to SSC training, as reflected by positive changes in muscle performance and muscle mass.

To determine whether muscles are capable of adapting to chronic high-intensity RTET at an old age, we maximally activated and exposed muscles of young and old rats to 80 SSCs, 2 days/wk (72 h between training bouts). These protocols were altered from our originally published proto-

Table 3. *Significantly differentially expressed genes relevant to PI3K-Akt and muscle growth for the tibialis anterior muscle following dorsiflexion SSC loading relative to nonloaded muscles*

			Young 3 days/wk		Young 2 days/wk		Old 3 days/wk		Old 2 days/wk	
Gene Symbol	Description	RefSeq No.	FC	*P* value	FC	*P* value	FC	*P* value	FC	*P* value
			Akt/PI3K family members and their regulators							
Akt2	V-akt murine thymoma viral oncogene homolog 2	NM_017093	↓1.38*	0.0173*	↓1.63*	0.0054*	↓1.20	0.1842	↓1.17	0.8244
Grb10	Growth factor receptor-bound protein-10	NM_001109093	↓1.31	0.2144	↓1.40*	0.0426*	↓1.22	0.5728	↑1.22	0.2888
Grb2	Growth factor receptor-bound protein-2	NM_030846	↓1.17	0.1810	↓1.17†	0.0819†	↓1.05	0.9621	↑1.11	0.4180
Hspb1	Heat shock protein-1	NM_031970	↑1.08	0.6024	↑2.07*	0.0011*	↓1.08	0.4440	↑2.16*	0.0398*
Ilk	Integrin-linked kinase	NM_133409	↓1.02	0.8547	↑1.00	0.9749	↑1.10	0.4336	↑1.29†	0.0993†
Mtcp1	Mature T cell proliferation 1	XM_001070795	↓1.59*	0.0358*	↓1.50*	0.0308*	↓1.42	0.1733	↓1.14	0.8505
Pdk2	Pyruvate dehydrogenase kinase, isozyme 2	NM_030872	↓1.45*	0.0046*	↓1.55*	0.0010*	↓1.31	0.3230	↓1.09	0.7266
Pdpk1	3-phosphoinositide-dependent protein kinase-1	NM_031081	↓1.26†	0.0759†	↓1.25*	0.0386*	↓1.14	0.3988	↑1.14	0.3459
Pi3k3r1	Phosphoinositide-3-kinase, regulatory subunit 1	NM_013005	↓1.43†	0.0565†	↓1.58*	0.0391*	↓1.42	0.1040	↓1.24	0.3978
Prkcz	Protein kinase Cζ	NM_022507	↓2.05*	0.0084*	↓1.98*	0.0017*	↓1.33	0.4962	↓1.56	0.2448
			Force transmission and mechanotransduction							
Itgb1	Integrin-β1	NM_017022	↑1.53*	0.0123*	↑1.95*	<0.0001*	↑1.70†	0.0775†	↑2.34*	0.0072*
Ptk2	PTK2 protein tyrosine kinase 2 (also known as focal adhesion kinase)	NM_013081	↓1.35*	0.0258*	↓1.43*	0.0106*	↓1.15	0.6602	↓1.03	0.7613
			IGF-1 signaling pathway							
Csnk2a1	Casein kinase 2, α1-polypeptide	NM_053824	↓1.20	0.2549	↓1.46†	0.0570†	↓1.13	0.8687	↓1.03	0.7479
Fos	FBJ osteosarcoma oncogene	NM_022197	↑1.47	0.4709	↑1.27	0.2837	↑2.57*	0.0458*	↑6.25*	0.0168*
Hras	Harvey rat sarcoma virus oncogene	NM_001098241	↓1.46*	0.0195*	↓1.21	0.1173	↓1.29	0.1931	↑1.09	0.4611
Irs1	Insulin receptor substrate 1	NM_012969	↑1.02	0.9168	↓1.11	0.5557	↓1.03	0.9305	↑1.53†	0.0777†
Jun	Jun oncogene	NM_021835	↑1.16	0.2424	↓2.36	0.6896	↓1.23†	0.0683†	↑1.57*	0.0241*
Map2k1	Mitogen-activated protein kinase 1	NM_031643	↓1.27	0.1934	↓1.27*	0.0253*	↓1.14	0.7504	↑1.01	0.6985
Mapk8	Mitogen-activated protein kinase 8	NM_053829	↓1.17	0.6829	↓1.77*	0.0022*	↓1.09	0.8617	↑1.13	0.4917
Raf1	V-raf-leukemia viral oncogene 1	NM_012639	↓1.21†	0.0614†	↓1.21†	0.0745†	↓1.08	0.8582	↑1.21	0.2527
Sos1	Son of sevenless homolog 1 (*Drosophila*)	NM_001100716	↓1.24*	0.0111*	↓1.23†	0.0636†	↓1.13	0.5640	↑1.11	0.4472
Ptpn11	Protein tyrosine phosphatase, nonreceptor type 11	NM_013088	↓1.37*	0.0128*	↓1.44*	0.0153*	↓1.25	0.4620	↑1.01	0.6772
Srf	Serum response factor (c-fos serum response element-binding transcription factor)	NM_001109302	↓1.18*	0.0188*	↓1.00	0.9511	↓1.10	0.8794	↑1.44†	0.0633†
			mTOR signaling pathway							
Eif4b	Eukaryotic translation initiation factor 4B	NM_001008324	↓1.25	0.1695	↓1.47*	0.0076*	↓1.21	0.3759	↑1.00	0.7125
Eif4e	Eukaryotic translation initiation factor 4E	NM_053974	↓1.20†	0.0839†	↓1.23*	0.0050*	↓1.07	0.8048	↑1.11	0.4189
Eif4ebp1	Eukaryotic translation initiation factor 4E-binding protein-1	NM_053857	↓1.47*	0.0225*	↓1.29*	0.0069*	↓1.16	0.3081	↓1.06	0.6880
Eif4g1	Eukaryotic translation initiation factor 4γ1		↓1.40	0.1074	↓1.52*	0.0145*	↓1.33	0.5250	↓1.13	0.7690
Fkbp1a	FK506-binding protein-1a	NM_013102	↓1.19*	0.0471*	↓1.09	0.2031	↑1.01	0.9536	↑1.10	0.3988
Mtor	Mechanistic target of rapamycin (serine/threonine kinase)	NM_019906	↓1.19	0.2779	↓1.27*	0.0329*	↓1.07	0.8875	↑1.15	0.3924
Rheb	Ras homolog enriched in brain	NM_013216	↑1.00	0.9960	↑1.17†	0.0672†	↓1.05	0.9051	↑1.41*	0.0341*
Rps6kb1	Ribosomal protein S6 kinase, polypeptide 1	NM_031985	↓1.17†	0.0939†	↓1.16	0.2515	↓1.04	0.9257	↑1.04	0.5851
Tsc1	Tuberous sclerosis 1	NM_021854	↓1.23	0.2577	↓1.36*	0.0325*	↓1.19	0.6980	↑1.11	0.4780
Tsc2	Tuberous sclerosis 2	NM_012680	↓1.29*	0.0173*	↓1.22*	0.0385*	↓1.28	0.1314	↓1.01	0.9511
			PI3K subunit genes and regulation of actin organization/cell migration							
Cdc42	Cell division cycle 42 (GTP-binding protein)	NM_171994	↓1.17*	0.0279*	↓1.14*	0.0426*	↓1.04	0.7280	↑1.12	0.2488
Pak1	P21 protein (Cdc42/Rac)-activated kinase 1	NM_017198	↑1.03	0.7088	↑1.39†	0.0603†	↑1.22	0.4118	↑1.42*	0.0022*
Rac1	Ras-related C3 botulinum toxin substrate 1	NM_134366	↓1.24*	0.0142*	↓1.19*	0.0171*	↓1.12	0.5877	↑1.06	0.5195
Wasl	Wiskott-Aldrich syndrome-like	NM_001110365	↓1.30†	0.0983†	↓1.24	0.1464	↓1.28	0.2234	↓1.08	0.8867

Continued

Table 3. *Continued*

Gene Symbol	Description	RefSeq No.	Young 3 days/wk		Young 2 days/wk		Old 3 days/wk		Old 2 days/wk	
			FC	*P* value	FC	*P* value	FC	*P* value	FC	*P* value
			Regulation of eIF4e and p70s6K							
Mapk1	Mitogen-activated protein kinase 1	NM_053842	↓1.15*	0.0309*	↓1.23*	0.0019*	↓1.03	0.8166	↑1.04	0.5864
Mapk14	Mitogen-activated protein kinase 14	NM_031020	↓1.51*	0.0110*	↓1.53*	0.0023*	↓1.34	0.2748	↓1.00	0.7664
Pabpc1	Poly(A)-binding protein, cytoplasmic 1	NM_134353	↑1.07	0.5336	↑1.17	0.1203	↑1.32*	0.0079*	↑1.39*	0.0063*
			Other PI3K-Akt signaling pathway genes							
Chuk	Conserved helix-loop-helix ubiquitous kinase	NM_001107588	↓1.15	0.1168	↓1.23†	0.0601†	↓1.07	0.8291	↑1.11	0.4602
			Inactivation of Gsk3 and accumulation of β-catenin							
Cd14	CD14 molecule	NM_021744	↑2.04	0.4715	↑2.69	0.2001	↑1.72†	0.0607†	↑1.52	0.1089
Ctnnb1	Catenin (cadherin-associated protein)-β1	NM_053357	↓1.22	0.1685	↓1.48*	0.0054*	↑1.28	0.7227	↓1.23	0.6579
Tirap	Toll-interleukin-1 receptor (TIR) domain-containing adaptor protein	XM_001055833	↓1.29*	0.0327*	↓1.49*	0.0211*	↓1.26	0.5200	↑1.05	0.5846
Tlr4	Toll-like receptor 4	NM_019178	↑1.35	0.2286	↑1.37†	0.0756†	↓1.27	0.9067	↑1.56†	0.0771†
Tollip	Toll-interacting protein	NM_001109668	↓1.13	0.6168	↓1.25†	0.0570†	↓1.27	0.6514	↓1.09	0.8961
			PTEN-dependent cell cycle arrest and apoptosis							
Cdkn1b	Cyclin-dependent kinase inhibitor 1B	NM_031762	↓1.28†	0.0570†	↓1.42*	0.0127*	↓1.07	0.8595	↑1.04	0.6191
Foxo3	Forkhead box O3	NM_001106395	↓1.35	0.2981	↓1.39*	0.0261*	↓1.18	0.4787	↓1.01	0.7489
Rbl2	Retinoblastoma-like 2	NM_031094	↓1.30*	0.0320*	↓1.36*	0.0132*	↓1.28	0.1827	↑1.24	0.7618
			BAD phosphorylation and antiapoptosis							
Ywhah	Tyrosine 3-monooxygenase/tryptophan 5-monooxygenase activation protein, η-polypeptide	NM_013052	↑1.07	0.5539	↑1.30*	0.0137*	↑1.19	0.2628	↑1.61*	0.0473*

Here, n = no. of rats; sample sizes were $n = 5–6$ per group; ↑ and ↓ indicate increased and decreased expression, respectively. BAD, Bcl2-associated agonist of cell death; FC, fold change; p70s6K, 70-kDa ribosomal protein S6 kinase; PI3K, phosphatidylinositol 3-kinase; PTEN, phosphatase and tensin homolog; RefSeq, National Center for Biotechnology Information Reference Sequence Database; SSC, stretch-shortening contraction. *Significantly differentially expressed genes that surpassed 1.1-fold change with a P value <0.05; †trend ($0.05 < P < 0.10$) for increased/decreased expression.

col (80 SSCs, 3 days/wk; 48 h between training bouts), in which young rats adapted and old rats maladapted (16). Similar to the response to 80 SSCs, 3 day/wk exposure, the modified exposure protocols induced muscle mass increases for Y3x, Y2x, and O2x. For young rats, the modified exposure protocol yielded similar gains in performance and muscle mass, indicating that muscles of young rats have the ability to adapt following a variety of SSC paradigms.

In the present study, O2x was superior over O3x as indicated by increases in muscle performance as well as improvements in muscle fiber area and MND that were similar to those of younger rodents. Our results indicating positive effects for 2 day/wk high-intensity RTET in older rodents are in line with a recent paper by Stec et al. (45), who found that 2 day/wk high-intensity training was beneficial for increasing muscle strength and performance compared with 3 day/wk (analogous to O3x) or 1 day/wk high-intensity training. Moreover, it should be noted that the authors found that 1 additional day of low-intensity training interspersed between 2 days of high-intensity training may elicit further benefits that may potentially maximize training benefits; this conclusion was based on a significantly greater thigh muscle mass compared with the other interventions, including the 2 day/wk high-intensity-only training. This would indicate that there are potential additional adaptive benefits when incorporating an extra day of low-intensity exercise into a training program that are absent with only the 2 days of high-intensity training represented in our present study. Unfortunately, given that we did not directly examine this exposure in the present study (i.e., 2 days/wk of high-intensity training separated by 1 day of low-intensity training), it is a limitation that we cannot directly compare O2x (i.e., 2 days/wk of high-intensity training) or O3x (i.e., 3 days/wk of high-intensity training) with the paradigm shown from the Stec et al. report, although it would certainly warrant examination in future research to confirm and elucidate the underlying integrated physiological processes supporting these findings. Indeed, with appreciation for the present molecular data described herein (i.e., RT^2 Profiler array gene expression, IPA, CNFs, and MNDs) as well as the positive results, namely that of muscle performance and muscle mass, that are complementary to those of the Stec et al. investigation, as well as other studies in humans (22–25, 29), our study provides support at a fundamental level that a reduced frequency of high-intensity RTET can be highly beneficial for aged muscle, particularly for those who do not respond favorably compared with higher frequencies of training. Additionally, the O2x paradigm in our study also falls in line with recent support for a "minimal-dose approach" of RTET of 2 days/wk of resistance exercise for <60 min that was based on previous research showing various physiological and psychological benefits to this type of training in older adults or the simple desire to achieve the benefits of RTET at a reduced time commitment (20).

The present data demonstrate that O2x was able to undergo adaptation concomitant with an enhanced activation of the PI3K-Akt pathway. Specifically, *Fos* and *Jun*, key regulators of satellite cell activation and migration involved during the myogenic process, were upregulated only in the O2x group. Fos and Jun dimerize together and form the transcription factor complex activator protein-1 (AP-1; 1, 12) and have been

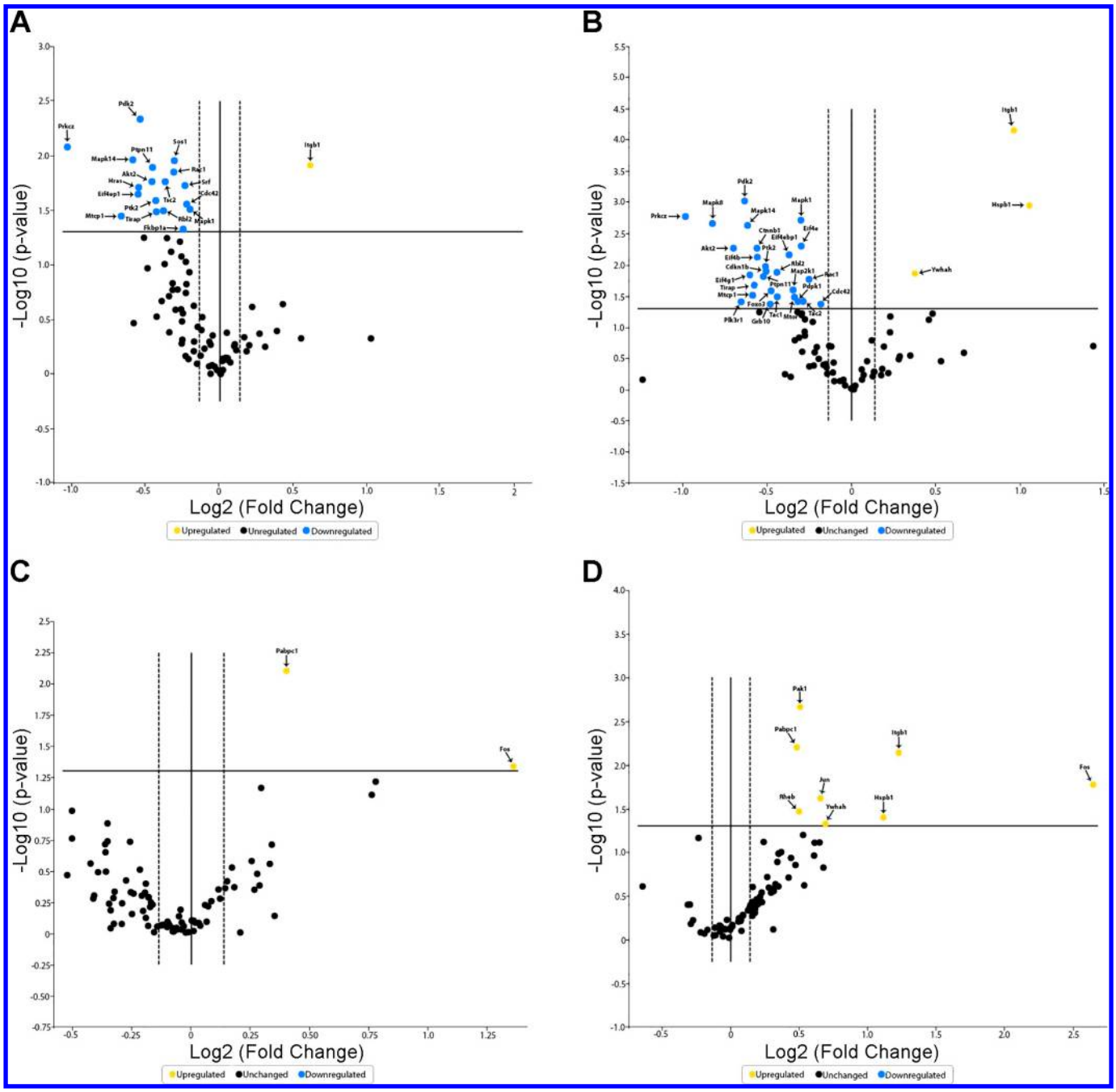

Fig. 4. Reduced frequency of stretch-shortening contraction (SSC) "resistance-type exercise" training increases phosphatidylinositol 3-kinase (PI3K)-Akt signaling in aged rats. The volcano plot graphs of the PI3K-Akt PCR array. These graphs show the log2 of the fold change for each gene's expression between SSC-loaded and nonloaded control tibialis anterior (TA) muscle for each group. Fold changes and *P* values were determined from comparisons of normalized cycle threshold (ΔC_t) values between SSC-loaded and nonloaded control TA muscles analyzed through the GeneGlobe Data Analysis Center (Qiagen): young rats trained 3 days/wk (*A*), young rats trained 2 days/wk (*B*), old rats trained 3 days/wk (*C*), and old rats trained 2 days/wk (*D*). Sample sizes were $n = 5–6$ per group. The vertical solid line indicates fold changes of 0. Vertical dashed lines indicate that the fold change in gene expression threshold is 1.1. The horizontal solid line indicates that the *P* value of the *t*-test threshold is 0.05. Genes that were significantly differentially expressed are labeled and colored according to whether they were upregulated or downregulated. See Table 3 for gene descriptors.

demonstrated to play a crucial role in the regulation of satellite cells during both myogenesis and skeletal muscle regeneration (1) as well as being involved in the control of muscle adaptation in response to exercise (12, 28, 31). Intriguingly, the top canonical pathway in the IPA for O2x was ERK/MAPK signaling. Thus, exercise variables that are prescribed in an appropriate manner for aged individuals, such as reducing the frequency, may provide evidence for an augmented systemic environment in aged skeletal muscle. However, these findings should be viewed within the perspective that we did not use traditional markers of satellite cell abundance, location, or function, such as paired box protein Pax-7 (Pax7) or myogenic determination protein (MyoD); because of the role of Fos and Jun in many other regulatory processes besides satellite cells,

Table 4. *Ingenuity Pathway Analysis of gene expression results from the PI3K-AKT Signaling Pathway RT² Profiler PCR Array for the tibialis anterior muscle following dorsiflexion SSC loading relative to nonloaded control muscles*

Analysis	Top 5 Results				
	Highest	Second highest	Middle	Second lowest	Lowest
			Young (3 mo) SSC loaded 3 days/wk		
Top canonical pathways (*P* value)	HGF signaling (6.90E−17)†	IGF-1 signaling (6.91E−15)†	FcεRI signaling (1.67E−14)†	PTEN signaling (3.47E−14)*	PI3K-Akt signaling (4.87E−14)†
Top networks (score)	Cell death and survival, cellular development, dermatological diseases and conditions (22)†	Cell death and survival, embryonic development, organismal development (6)†	Cell-to-cell signaling and interaction, nervous system development and function, carbohydrate metabolism (6)†	Cell death and survival, cell morphology, cellular assembly and organization (6)†	N/A
Top merged-network functions (bias-corrected activation *z*-score)	Cell death and survival (apoptosis of kidney cell lines) (2.419)*	Cell death and survival (cell death of immune cells) (−2.010)†	Carbohydrate metabolism (uptake of monosaccharide) (−1.916)†	Cellular development, cellular growth and proliferation, embryonic development (proliferation of embryonic cell lines) (−1.736)†	Cell cycle, gene expression (binding of protein binding site) (−1.729)‡
			Young (3 mo) SSC loaded 2 days/wk		
Top canonical pathways (*P* value)	PI3K-Akt signaling (5.01E−29)†	Insulin receptor signaling (3.36E−26)†	IGF-1 signaling (2.48E−21)†	PTEN signaling (2.93E−20)*	mTOR signaling (9.60E−20)†
Top networks (score)	Protein synthesis, cell morphology, cellular function and maintenance (25)†	Cell cycle, connective tissue development and function, cardiac proliferation (12)†	Developmental disorder, neurological disease, connective tissue disorders (10)†	Cellular movement, cell death and survival, skeletal and muscular system development and function (7)†	Cellular development, cell-to-cell signaling and interaction, cellular assembly and organization (3)†
Top merged-network functions (bias-corrected activation *z*-score)	Cellular development, cellular growth and proliferation (proliferation of stem cells) (2.246)*	Carbohydrate metabolism (uptake of monosaccharide) (−2.138)†	Cell death and survival (apoptosis of leukocyte cell lines) (−2.119)†	Cell death and survival (cell death of immune cells) (−2.007)†	Cellular development, cellular growth and proliferation, hematological system development and function, inflammatory response, lymphoid tissue structure and development (proliferation of phagocytes) (1.953)*
			Old (30 mo) SSC loaded 3 days/wk		
Canonical pathways (*P* value)	IL-17A signaling in gastric cells (2.40E−03)†	Antiproliferative role of TOB in T cell signaling (2.49E−03)†	TNFR2 signaling (2.78E−03)‡	IL-17A signaling in fibroblasts (3.36E−03)†	April-mediated signaling (3.64E−03)‡
Top network (score)	Protein synthesis, cell death and survival, RNA posttranscriptional modification (6)*				
Top merged-network functions (*z*-score)	N/A	N/A	N/A	N/A	N/A
			Old (30 mo) SSC loaded 2 days/wk		
Canonical pathways (*P* value)	ERK/MAPK signaling (3.02E−09)*	HGF signaling (4.19E−08)*	Cdc42 signaling (2.72E−07)*	TNFR1 signaling (6.78E−07)‡	Signaling by Rho family GTPases (1.05E−06)*
Top networks (score)	Cellular development, cell death and survival, skeletal and muscular system development and function (10)*	Behavior, cell death and survival, cellular compromise (10)*			
Top merged-network functions (bias-corrected activation *z*-score)	Protein synthesis (expression of protein) (1.569)*	Cellular development, cellular growth and proliferation, connective tissue development (cell proliferation of fibroblasts) (1.257)*	Cardiovascular system development and function, organismal development (angiogenesis) (1.193)*	Cellular development, cellular growth and proliferation, connective tissue development and function (proliferation of fibroblast cell lines) (0.687)*	Cellular development, cellular growth and proliferation, hair and skin development and function, organ development, tissue development (proliferation of epidermal cell lines) (0.639)*

P values (for top canonical pathways), scores (for top networks), and bias-corrected activation *z*-scores (for top merged-network functions) are in parentheses; n = no. of rats. The top 5 results from each category are included in the table. All Ingenuity Pathway Analysis functions with the exception of cancer-specific, reproductive system, and psychological functions were considered for this table. Sample sizes were $n = 5–6$ per group. Cdc42, cell division cycle 42; FcεRI, high-affinity IgE receptor; HGF, hepatocyte growth factor; mTOR, mechanistic target of rapamycin; N/A, not available; PI3K, phosphatidylinositol 3-kinase; PTEN, phosphatase and tensin homolog; SSC, stretch-shortening contraction; TNFR, TNF receptor; TOB, transducer of ErbB2; 6.90E−17, 6.90×10^{-17}. For top canonical pathways and top networks, activation state is based on the number of genes associated with the pathway array that were upregulated or downregulated, and for top merged-network functions, activation state is based on *z*-score: *increased activation; †decreased activation; ‡unchanged.

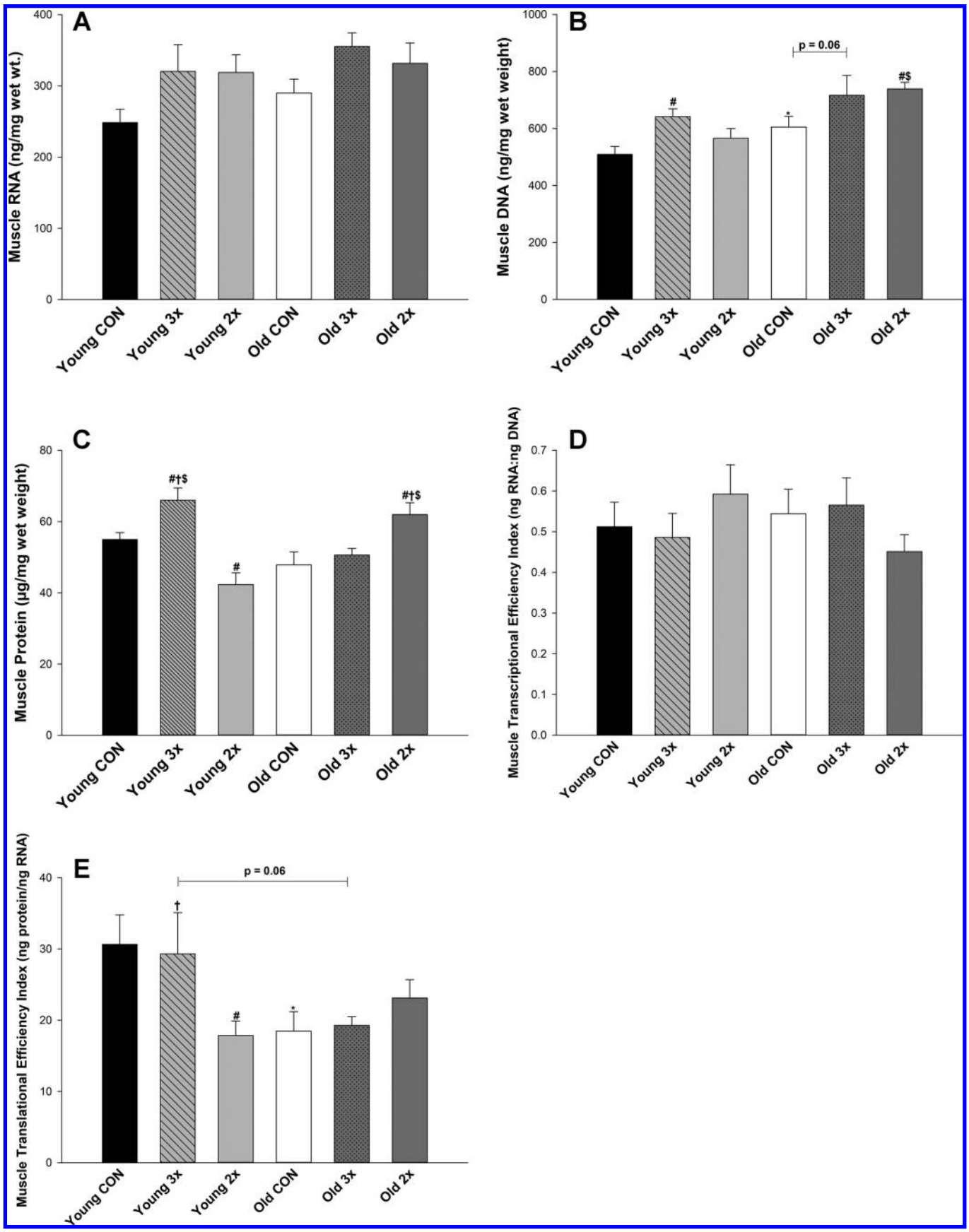
A
Muscle RNA (ng/mg wet wt.)
400
300
200
100
0
Young CON
Young 3x
Young 2x
Old CON
Old 3x
Old 2x
B
Muscle DNA (ng/mg wet weight)
1000
800
600
400
200
0
p = 0.06
#
*
#$
C
Muscle Protein (µg/mg wet weight)
80
60
40
20
0
#†$
#
#†$
D
Muscle Transcriptional Efficiency Index (ng RNA:ng DNA)
0.7
0.6
0.5
0.4
0.3
0.2
0.1
0.0
E
Muscle Translational Efficiency Index (ng protein/ng RNA)
40
30
20
10
0
p = 0.06
†
#
*

this response will have to be assessed in future studies to confirm these findings.

Itgb1, a molecule crucial for mechanotransduction signaling of Akt, independent of growth factor or nutrient factors (26), was upregulated only in Y3x, Y2x, and O2x (Table 3). In response to mechanical activation, *Itgb1* signals to integrin-linked kinase (ILK), leading to the subsequent activation of mTOR; mTOR subsequently increases protein synthesis, ribosomal biogenesis, and eventual muscle growth (11, 32, 46). Moreover, through canonical PI3K signaling, ILK works in concert with pyruvate dehydrogenase kinase 1 to stimulate Akt, eventually leading to increased protein synthesis and expression of genes related to growth and remodeling in skeletal muscle (11). Interestingly, the IPA revealed that adapted groups have higher activation states of pathways related to PI3K canonical signaling, such as ERK/MAPK, HGF, IGF-1, and mTOR (Table 4). Thus, the results of the present study indicate that RTET that promotes adaptation (i.e., Y3x, Y2x, and O2x) enhances mechanotransduction signaling through *Itgb1*, subsequently increasing muscle protein content and skeletal muscle fiber area.

The PI3K-Akt signaling pathway has been shown to stimulate and control the activity of multiple functional processes, including protein synthesis, glucose uptake, glycogen synthesis, cell cycle progression, cell growth, and an inhibition of apoptosis (21). Therefore, modulation of genes and proteins within this pathway has a crucial role in integrating both anabolic and catabolic signals, ultimately leading to changes in myofiber area and overall muscle mass. In the present study, we have shown that appropriate, age-specific RTET (i.e., Y3x, Y2x, and O2x) leads to increased expression of PI3K-Akt genes as reflected by the RT^2 Profiler arrays and bioinformatics analysis via IPA, whereas a dysregulated response occurs in O3x. This is an important distinction because these observations suggest that SSC loading, when prescribed in the appropriate manner, directly modifies local PI3K-Akt activity within skeletal muscle, which improves cellular metabolism and leads to an adaptive fate. Therefore, reducing the frequency of RTET, thereby allowing additional recovery time to initiate muscle repair and remodeling processes, provides an optimal environment for aged muscle to adapt properly and aids in restoring muscle performance and physiology as well as the microenvironment, subsequently improving soft-tissue quality and functional outcomes with advanced age.

Although we believe that the results from the present study provide valuable information about optimizing the spacing of exercise in an old versus young state, there are limitations. First, our study was limited to two age groups, which consisted of young (3 mo) and old (30 mo) rats that were SSC loaded 3 or 2 days/wk. Recent literature suggests that age-related declines may potentially occur much sooner than what would be expected, potentially before any overt symptoms of the onset of chronic disease (13, 40), which indicates that testing intermediate age groups is critical (35, 42). Moreover, our findings of no differences in muscle mass wet weight between young and old NLC may also be due to a lack of intermediate age groups; 3-mo-old rats (comparable to 16–20-yr-old humans) are at late adolescence/young adulthood, before they reach their adult weight. Previous research from our laboratory has demonstrated that 6–9-mo-old F344xBN rats, but not 3-mo-old rats, have significantly less NLC muscle relative to 26–33-mo-old rodents (18, 35). Emphasizing our previous work (6, 16, 36), the basis for choosing 3-mo-old rats was to select a population that had the highest potential in terms of adaptability to high-intensity SSC RTET as well as serving as a representative age group for a young occupational demographic. Importantly, our findings of significantly enhanced muscle performance and muscle fiber areas (Figs. 1 and 2) still provide a fundamental basis for the use of appropriately prescribed RTET in preventing the onset of age-associated sarcopenia and/or dynapenia.

Next, the study was limited by investigating only rats, and not humans. Although using the F344xBN rats allowed for finding important molecular findings that are driving muscle adaptation (e.g., gene expression of signaling pathways, etc.), caution should be used in directly translating the findings to humans. However, it is noteworthy that in a recent review, Ballak et al. (8), after an extensive review of the literature, found that the model used in the present study, F344xBN, most closely resembled the aging of muscle in men more so than any other animal model they examined.

Another limitation to the present study was that we did not look at fiber type distribution. In a previous study by our laboratory (35), we showed that in younger rodents subjected to 3 day/wk chronic SSC RTET there was a significant shift in fiber type distribution from type IIb to type IIx fibers, whereas old rats that maladapted had a blunted fiber type shift response. Overall, in younger rodents, the high-intensity training of the present model that is intended to target type II fibers resulted in a more oxidative phenotype, explaining the ability to recover from fatigue. This suggests that the shift in fiber type distribution could be playing a role in the adaptive or maladaptive response to SSC training. Although not looked at in the present study, a future research question is what the fiber type distribution would look like in O2x following chronic RTET. We would speculate on the basis of the present data and past research by our laboratory (35, 36) that this group would have fiber type distribution shift that looks more similar to that of young rats that adapted to the 3 day/wk loading paradigm; this needs to be confirmed in future studies. Finally, although it was outside the scope of this study, only signaling events associated with growth and remodeling were investigated, while excluding pathways involved in the stress response to exercise that also underlies muscle adaptation, such as apoptosis, reactive

Fig. 5. Reduced frequency of stretch-shortening contraction "resistance-type exercise" training augments muscle DNA, protein, and translational efficiency in aged rats. Comparison of the molecular attributes between young and old rodent skeletal muscle for muscle RNA (*A*), muscle DNA (*B*), muscle protein (*C*), transcriptional efficiency index (RNA-to-DNA ratio; *D*), and translational efficiency index (protein-to-RNA ratio; *E*). Both RNA and DNA concentrations were obtained using a spectrophotometer (ND-1000; NanoDrop Technologies). Total protein contents of the cytoplasmic protein extracts were quantified and reported as protein concentration (μg protein/mg tissue). The transcriptional efficiency index and translational efficiency index are surrogate measures of global transcriptional and translational efficiency and have been used previously (40). *Different from Young CON, $P < 0.05$; #different from nonloaded control (CON) within age, $P < 0.05$; †different from treatment within age, $P < 0.05$; $different from treatment by age, $P < 0.05$.

oxygen species metabolism, and autophagy (3, 33). Of note, IPA (Table 4) indicated that cell death and survival constituted a highly expressed functional outcome in the adaptive groups; thus, investigating the stress response following modification of variables involving the RTET prescription with aging is warranted in future research.

In conclusion, we provide key insights into the growth and remodeling signaling response in skeletal muscle to appropriately prescribed, age-specific RTET involving PI3K-Akt pathway expression, which partially underlies training adaptation with aging. Aged skeletal muscle demonstrates an impairment in the ability to adapt properly to chronic SSC RTET when conducted at a higher frequency; however, when reducing the frequency of exercise, old muscle can adapt through enhanced muscle performance and increased muscle fiber areas. Additionally, these features are supported by a concomitant improvement in the growth and remodeling molecular environment, specifically the PI3K-Akt pathway, that promotes central nucleation and MND remodeling, and partially explains the underlying basis for adaptive outcomes in aged rodents following RTET. Thus, the findings in the present study support the notion that age-appropriate exercise prescription, in this case reducing the frequency of training in aged rodents, reverses age-associated negative alterations in key pathways involved in growth and remodeling of skeletal muscle and rejuvenates the systemic environment in a favorable manner that results in muscle adaptation. Future studies should focus on interrogating the fundamental aspects of additional RTET prescriptions for maximizing potential benefits as well as revealing additional molecular influences (e.g., gene signaling, DNA methylation, etc.) that affect muscle adaptation occurring with RTET and how they are influenced by titrating the parameters of the exercise prescription.

GRANTS

This work was supported by Centers for Disease Control and Prevention National Institute for Occupational Safety and Health Grant CDC/NIOSH-6939050.

DISCLAIMERS

The findings and conclusions in this report are those of the authors and do not necessarily represent the official position of the National Institute for Occupational Safety and Health, Centers for Disease Control and Prevention.

DISCLOSURES

No conflicts of interest, financial or otherwise, are declared by the authors.

AUTHOR CONTRIBUTIONS

M.A.N., E.P.R., J.E., M.L.K., and B.A.B. conceived and designed research; M.A.N., E.P.R., J.E., and B.A.B. performed experiments; M.A.N., M.L.K., and B.A.B. analyzed data; M.A.N. and B.A.B. interpreted results of experiments; M.A.N. and B.A.B. prepared figures; M.A.N. and B.A.B. drafted manuscript; M.A.N., E.P.R., and B.A.B. edited and revised manuscript; M.A.N., E.P.R., J.E., M.L.K., and B.A.B. approved final version of manuscript.

REFERENCES

1. **Alli NS, Yang EC, Miyake T, Aziz A, Collins-Hooper H, Patel K, McDermott JC.** Signal-dependent fra-2 regulation in skeletal muscle reserve and satellite cells. *Cell Death Dis* 4: e692, 2013. doi:10.1038/cddis.2013.221.
2. **Almada AE, Wagers AJ.** Molecular circuitry of stem cell fate in skeletal muscle regeneration, ageing and disease. *Nat Rev Mol Cell Biol* 17: 267–279, 2016. doi:10.1038/nrm.2016.7.
3. **Alway SE.** Inflammation and oxidative stress limit adaptation to stretch-shortening contractions in aging. *Exerc Sport Sci Rev* 45: 194, 2017. doi:10.1249/JES.0000000000000126.
4. **Baker BA, Cutlip RG.** Skeletal muscle injury versus adaptation with aging: novel insights on perplexing paradigms. *Exerc Sport Sci Rev* 38: 10–16, 2010. doi:10.1097/JES.0b013e3181c5cd7c.
5. **Baker BA, Hollander MS, Kashon ML, Cutlip RG.** Effects of glutathione depletion and age on skeletal muscle performance and morphology following chronic stretch-shortening contraction exposure. *Eur J Appl Physiol* 108: 619–630, 2010. doi:10.1007/s00421-009-1258-4.
6. **Baker BA, Hollander MS, Mercer RR, Kashon ML, Cutlip RG.** Adaptive stretch-shortening contractions: diminished regenerative capacity with aging. *Appl Physiol Nutr Metab* 33: 1181–1191, 2008. doi:10.1139/H08-110.
7. **Baker BA, Mercer RR, Geronilla KB, Kashon ML, Miller GR, Cutlip RG.** Stereological analysis of muscle morphology following exposure to repetitive stretch-shortening cycles in a rat model. *Appl Physiol Nutr Metab* 31: 167–179, 2006. doi:10.1139/h05-009.
8. **Ballak SB, Degens H, de Haan A, Jaspers RT.** Aging related changes in determinants of muscle force generating capacity: a comparison of muscle aging in men and male rodents. *Ageing Res Rev* 14: 43–55, 2014. doi:10.1016/j.arr.2014.01.005.
9. **Bamman MM, Cooper DM, Booth FW, Chin ER, Neufer PD, Trappe S, Lightfoot JT, Kraus WE, Joyner MJ.** Exercise biology and medicine: innovative research to improve global health. *Mayo Clin Proc* 89: 148–153, 2014. doi:10.1016/j.mayocp.2013.11.013.
10. **Boppart MD, Burkin DJ, Kaufman SJ.** $\alpha_7\beta_1$-Integrin regulates mechanotransduction and prevents skeletal muscle injury. *Am J Physiol Cell Physiol* 290: C1660–C1665, 2006. doi:10.1152/ajpcell.00317.2005.
11. **Burkholder TJ.** Mechanotransduction in skeletal muscle. *Front Biosci* 12: 174–191, 2007. doi:10.2741/2057.
12. **Caldow MK, Steinberg GR, Cameron-Smith D.** Impact of SOCS3 overexpression on human skeletal muscle development in vitro. *Cytokine* 55: 104–109, 2011. doi:10.1016/j.cyto.2011.03.012.
13. **Cooper R, Bann D, Wloch EG, Adams JE, Kuh D.** "Skeletal muscle function deficit" in a nationally representative British birth cohort in early old age. *J Gerontol A Biol Sci Med Sci* 70: 604–607, 2015. doi:10.1093/gerona/glu214.
14. **Crawford JO, Graveling RA, Cowie HA, Dixon K.** The health safety and health promotion needs of older workers. *Occup Med (Lond)* 60: 184–192, 2010. doi:10.1093/occmed/kqq028.
15. **Cristea A, Qaisar R, Edlund PK, Lindblad J, Bengtsson E, Larsson L.** Effects of aging and gender on the spatial organization of nuclei in single human skeletal muscle cells. *Aging Cell* 9: 685–697, 2010. doi:10.1111/j.1474-9726.2010.00594.x.
16. **Cutlip RG, Baker BA, Geronilla KB, Mercer RR, Kashon ML, Miller GR, Murlasits Z, Alway SE.** Chronic exposure to stretch-shortening contractions results in skeletal muscle adaptation in young rats and maladaptation in old rats. *Appl Physiol Nutr Metab* 31: 573–587, 2006. doi:10.1139/h06-033.
17. **Cutlip RG, Stauber WT, Willison RH, McIntosh TA, Means KH.** Dynamometer for rat plantar flexor muscles in vivo. *Med Biol Eng Comput* 35: 540–543, 1997. doi:10.1007/BF02525537.
18. **Degens H, Alway SE.** Skeletal muscle function and hypertrophy are diminished in old age. *Muscle Nerve* 27: 339–347, 2003. doi:10.1002/mus.10314.
19. **Evans WJ.** What is sarcopenia? *J Gerontol A Biol Sci Med Sci* 50: 5–8, 1995. doi:10.1093/gerona/50A.Special_Issue.5.
20. **Fisher JP, Steele J, Gentil P, Giessing J, Westcott WL.** A minimal dose approach to resistance training for the older adult; the prophylactic for aging. *Exp Gerontol* 99: 80–86, 2017. doi:10.1016/j.exger.2017.09.012.
21. **Frost RA, Lang CH.** Protein kinase B/Akt: a nexus of growth factor and cytokine signaling in determining muscle mass. *J Appl Physiol (1985)* 103: 378–387, 2007. doi:10.1152/japplphysiol.00089.2007.
22. **Hagerman FC, Walsh SJ, Staron RS, Hikida RS, Gilders RM, Murray TF, Toma K, Ragg KE.** Effects of high-intensity resistance training on untrained older men. I. Strength, cardiovascular, and metabolic responses. *J Gerontol A Biol Sci Med Sci* 55: B336–B346, 2000. doi:10.1093/gerona/55.7.B336.
23. **Häkkinen K, Kraemer WJ, Newton RU, Alen M.** Changes in electromyographic activity, muscle fibre and force production characteristics during heavy resistance/power strength training in middle-aged and older men and women. *Acta Physiol Scand* 171: 51–62, 2001. doi:10.1046/j.1365-201x.2001.171001051.x.

24. **Häkkinen K, Pakarinen A, Kraemer WJ, Häkkinen A, Valkeinen H, Alen M.** Selective muscle hypertrophy, changes in EMG and force, and serum hormones during strength training in older women. *J Appl Physiol (1985)* 91: 569–580, 2001. doi:10.1152/jappl.2001.91.2.569.
25. **Hikida RS, Staron RS, Hagerman FC, Walsh S, Kaiser E, Shell S, Hervey S.** Effects of high-intensity resistance training on untrained older men. II. Muscle fiber characteristics and nucleo-cytoplasmic relationships. *J Gerontol A Biol Sci Med Sci* 55: B347–B354, 2000. doi:10.1093/gerona/55.7.B347.
26. **Hornberger TA, Esser KA.** Mechanotransduction and the regulation of protein synthesis in skeletal muscle. *Proc Nutr Soc* 63: 331–335, 2004. doi:10.1079/PNS2004357.
27. **Hornberger TA, Stuppard R, Conley KE, Fedele MJ, Fiorotto ML, Chin ER, Esser KA.** Mechanical stimuli regulate rapamycin-sensitive signalling by a phosphoinositide 3-kinase-, protein kinase B- and growth factor-independent mechanism. *Biochem J* 380: 795–804, 2004. doi:10.1042/bj20040274.
28. **LaFramboise WA, Jayaraman RC, Bombach KL, Ankrapp DP, Krill-Burger JM, Sciulli CM, Petrosko P, Wiseman RW.** Acute molecular response of mouse hindlimb muscles to chronic stimulation. *Am J Physiol Cell Physiol* 297: C556–C570, 2009. doi:10.1152/ajpcell.00046.2009.
29. **Melov S, Tarnopolsky MA, Beckman K, Felkey K, Hubbard A.** Resistance exercise reverses aging in human skeletal muscle. *PLoS One* 2: e465, 2007. doi:10.1371/journal.pone.0000465.
30. **Naimo MA, Gu JK, Lilly C, Kelley GA, Baker BA.** Resistance training frequency confers greater muscle quality in aged individuals: a brief NHANES report. *JCSM Clin Rep* 3: 64, 2018. doi:10.17987/jcsm-cr.v3i2.64.
31. **Nikolaidis MG, Papazisis KT, Kortsaris AH, Mougios V.** Exercise-induced changes in c-Fos protein levels in skeletal muscle of trained and untrained rats. *Int J Sports Med* 24: 96–100, 2003. doi:10.1055/s-2003-38198.
32. **Philp A, Hamilton DL, Baar K.** Signals mediating skeletal muscle remodeling by resistance exercise: PI3-kinase independent activation of mTORC1. *J Appl Physiol (1985)* 110: 561–568, 2011. doi:10.1152/japplphysiol.00941.2010.
33. **Quadrilatero J, Alway SE, Dupont-Versteegden EE.** Skeletal muscle apoptotic response to physical activity: potential mechanisms for protection. *Appl Physiol Nutr Metab* 36: 608–617, 2011. doi:10.1139/h11-064.
34. **Rader EP, Baker BA.** Inflammaging and the age-specific responsiveness to stretch-shortening contractions. *Exerc Sport Sci Rev* 45: 195–200, 2017. doi:10.1249/JES.0000000000000123.
35. **Rader EP, Layner K, Triscuit AM, Chetlin RD, Ensey J, Baker BA.** Age-dependent muscle adaptation after chronic stretch-shortening contractions in rats. *Aging Dis* 7: 1–13, 2016. doi:10.14336/AD.2015.0920.
36. **Rader EP, Naimo MA, Layner KN, Triscuit AM, Chetlin RD, Ensey J, Baker BA.** Enhancement of skeletal muscle in aged rats following high-intensity stretch-shortening contraction training. *Rejuvenation Res* 20: 93–102, 2017. doi:10.1089/rej.2016.1816.
37. **Raue U, Slivka D, Jemiolo B, Hollon C, Trappe S.** Proteolytic gene expression differs at rest and after resistance exercise between young and old women. *J Gerontol A Biol Sci Med Sci* 62: 1407–1412, 2007. doi:10.1093/gerona/62.12.1407.
38. **Raue U, Slivka D, Minchev K, Trappe S.** Improvements in whole muscle and myocellular function are limited with high-intensity resistance training in octogenarian women. *J Appl Physiol (1985)* 106: 1611–1617, 2009. doi:10.1152/japplphysiol.91587.2008.
39. **Raue U, Trappe TA, Estrem ST, Qian HR, Helvering LM, Smith RC, Trappe S.** Transcriptome signature of resistance exercise adaptations: mixed muscle and fiber type specific profiles in young and old adults. *J Appl Physiol (1985)* 112: 1625–1636, 2012. doi:10.1152/japplphysiol.00435.2011.
40. **Roberts MD, Kerksick CM, Dalbo VJ, Hassell SE, Tucker PS, Brown R.** Molecular attributes of human skeletal muscle at rest and after unaccustomed exercise: an age comparison. *J Strength Cond Res* 24: 1161–1168, 2010. doi:10.1519/JSC.0b013e3181da786f.
41. **Ryan MJ, Dudash HJ, Docherty M, Geronilla KB, Baker BA, Haff GG, Cutlip RG, Alway SE.** Aging-dependent regulation of antioxidant enzymes and redox status in chronically loaded rat dorsiflexor muscles. *J Gerontol A Biol Sci Med Sci* 63: 1015–1026, 2008. doi:10.1093/gerona/63.10.1015.
42. **Sharples AP, Stewart CE, Seaborne RA.** Does skeletal muscle have an 'epi'-memory? The role of epigenetics in nutritional programming, metabolic disease, aging and exercise. *Aging Cell* 15: 603–616, 2016. doi:10.1111/acel.12486.
43. **Siu PM, Bryner RW, Martyn JK, Alway SE.** Apoptotic adaptations from exercise training in skeletal and cardiac muscles. *FASEB J* 18: 1150–1152, 2004. doi:10.1096/fj.03-1291fje.
44. **Slivka D, Raue U, Hollon C, Minchev K, Trappe S.** Single muscle fiber adaptations to resistance training in old (>80 yr) men: evidence for limited skeletal muscle plasticity. *Am J Physiol Regul Integr Comp Physiol* 295: R273–R280, 2008. doi:10.1152/ajpregu.00093.2008.
45. **Stec MJ, Thalacker-Mercer A, Mayhew DL, Kelly NA, Tuggle SC, Merritt EK, Brown CJ, Windham ST, Dell'Italia LJ, Bickel CS, Roberts BM, Vaughn KM, Isakova-Donahue I, Many GM, Bamman MM.** Randomized, four-arm, dose-response clinical trial to optimize resistance exercise training for older adults with age-related muscle atrophy. *Exp Gerontol* 99: 98–109, 2017. doi:10.1016/j.exger.2017.09.018.
46. **Yamada AK, Verlengia R, Bueno Junior CR.** Mechanotransduction pathways in skeletal muscle hypertrophy. *J Recept Signal Transduct Res* 32: 42–44, 2012. doi:10.3109/10799893.2011.641978.